Frontiers in Bioscience Landmark

Front. Biosci. (Landmark Ed) **2022**; 27(8): 237
https://doi.org/10.31083/j.fbl2708237

Original Research

Dynamics of Acute Liver Injury in Experimental Models of Hepatotoxicity in the Context of Their Implementation in Preclinical Studies on Stem Cell Therapy

Piotr Czekaj[1,*,†], Mateusz Król[1,†], Łukasz Limanówka[2], Aleksandra Skubis-Sikora[1], Emanuel Kolanko[1], Edyta Bogunia[1], Mateusz Hermyt[1], Marcin Michalik[1], Bartosz Sikora[1], Agnieszka Prusek[1], Aniela Grajoszek[3], Jacek Pająk[4]

[1]Department of Cytophysiology, Chair of Histology and Embryology, Faculty of Medical Sciences in Katowice, Medical University of Silesia in Katowice, 40-752 Katowice, Poland
[2]Students Scientific Society, Chair of Histology and Embryology, Faculty of Medical Sciences in Katowice, Medical University of Silesia in Katowice, 40-752 Katowice, Poland
[3]Department of Experimental Medicine, Medical University of Silesia in Katowice, 40-752 Katowice, Poland
[4]Department of Pathomorphology and Molecular Diagnostic, Faculty of Medical Sciences in Katowice, Medical University of Silesia in Katowice, 40-752 Katowice, Poland
*Correspondence: pcz@sum.edu.pl (Piotr Czekaj)
[†]These authors contributed equally.
Academic Editor: Gustavo Yannarelli
Submitted: 20 May 2022 Revised: 2 July 2022 Accepted: 22 July 2022 Published: 10 August 2022

Abstract

Background and Aims: Experimental models using carbon tetrachloride (CCl_4) and D-galactosamine (D-GalN) can be used in preclinical assessment of acute liver failure (ALF) therapies. Unfortunately, these models are characterized by different dynamics of liver injury depending on the animal strain, administered hepatotoxin, and its dose. The aim of this study was to compare known rat and mouse models of ALF with a view to their future introduction into preclinical cell therapy experiments. In particular, based on histopathological and molecular changes, we suggested experimental time cut-off points for an effective stem cell therapeutic intervention. **Methods**: ALF was induced by a single intraperitoneal injection of CCl_4 in mice (50 μL/100 g b.w.) and rats (200 μL/100 g b.w.) and D-GalN in mice (150 mg/100 g b.w.) and rats (50 mg/100 g b.w.). Blood and liver samples were collected 12 h, 24 h, 48 h and 7 days after intoxication. Blood morphology, liver function blood tests, histopathological changes, proliferation activity, apoptosis, fibrosis, and gene expression were analysed to assess liver damage. **Results**: At 12 h, 24 h, and 48 h after CCl_4 injection, mouse livers showed moderate inflammatory infiltration and massive pericentral necrosis. In rats treated with CCl_4, minor lymphocytic infiltration in the liver parenchyma was seen at 12 h, followed by necrosis that appeared around central veins at 24 h and persisted to 48 h. In D-GalN-injected mice, the first histopathological signs of liver injury appeared at 48 h. In the livers of D-GalN-treated rats, moderate pericentral inflammatory infiltration occurred after 12 h, 24 h, and 48 h, accompanied by increased proliferation and apoptosis. All histological changes were accompanied by decreasing expression of certain genes. In most experimental groups of rats and mice, both histological and molecular parameters returned to the baseline values between 48 h and 7 days after intoxication. **Conclusions**: In mice and rats with CCl_4-induced ALF, signs of liver failure can be seen as early as 12 h and develop to 48 h. In the D-GalN-induced model, mice are more resistant to the hepatotoxic effect than rats (after 12 h), and the early hepatitis phase can be observed much later, after 48 h. These cut-off points seem to be optimal for suppressing inflammation and applying effective stem cell therapy for acute liver injury.

Keywords: experimental models of hepatotoxicity; galactosamine; carbon tetrachloride; acute liver failure; stem cell therapy

1. Introduction

Acute liver failure (ALF) is a serious disease defined as destruction of parenchymal tissue accompanied by the impairment of protein synthesis and detoxifying function, reflected by the presence of jaundice, coagulopathy and liver encephalopathy within short period of time after first symptoms appeared. Liver dysfunction results from potentially reversible liver parenchyma necrosis which is most often caused by viral infection or acetaminophen overdose [1]. Despite reversibility of the disease, it is associated with a high mortality rate. Depending on the aetiology, in the mild course of ALF, it can be effectively treated causally as in acetaminophen overdose, where acetylcysteine can be administered as an antidote. In acute hepatotropic viral infections and different drug overdoses, there is no effective causal treatment, therefore symptomatic treatment is applied [2]. Patients with mild to moderate onset of ALF are usually treated in internal medicine or paediatric wards, where medical management includes prevention of liver failure complications, fluid therapy, and pharmacological liver supportive treatments, such as ornithine administration [3]. In fulminant or hyperacute course of the

disease, the only therapeutic option is liver transplantation [4]. However, organ transplantation has important drawbacks including high cost, low organ availability, the necessarily of using life-long immunosuppression treatment and risk of multiple complications [1,5,6]. In view of the donor shortage, the need for immunosuppressive treatment, and post-transplant complications, there is imperative to develop a new alternative therapy capable of improving the clinical condition of patients, reducing mortality, or prolonging patient survival [7]. Stem cell-based therapy may be a promising alternative or adjuvant treatment to the currently used methods [8–11]. Cell therapies with bone marrow mesenchymal stem cells (BM-MSCs) [12], Wharton's jelly mesenchymal stem cells (WJ-MSCs) [13], hepatocyte-like cells derived from human amniotic epithelial cells (hAEC-HLCs) [14], and hepatocyte-like cells derived from induced pluripotent stem cells (iPS-HLCs) [15] have been proven effective in animal models of ALF. Implanted cells could partially take over the function of damaged liver parenchyma (e.g., hepatocyte implantation) [16], increase liver regenerative ability (e.g., mesenchymal stem cells implantation) [17,18] or suppress destructive inflammatory reaction (e.g., amniotic epithelial and mesenchymal cells implantation) [19,20]. It is also suggested that the mechanism of therapeutic action of the above-mentioned cells may be more related to the secreted paracrine factors and microvesicles than to the transplanted cells themselves [21,22].

Experimental mouse and rat models of ALF using carbon tetrachloride (CCl_4) and D-galactosamine (D-GalN) allow observation of the progression of liver diseases, particularly those observations that cannot be performed in patients for ethical and medical reasons [23,24]. Therefore, animal models of induced hepatotoxicity can be used in the preclinical assessment of acute and chronic liver injury therapies. Unfortunately, the various mechanisms of xenobiotic toxicity and different sensitivity of animal species and strains to intoxication result in different intoxication effects and, as a consequence, some difficulties in data interpretation and extrapolation to humans [24]. Additionally, different approaches to liver injury assessment make it difficult to perform comparative analysis and choose the optimal *in vivo* model [23].

The main mechanism of liver injury by CCl_4 involves its biotransformation resulting in free radical generation, i.e., CCl_3, cell membrane oxidation, and DNA damage [25]. Free radicals are generated by cytochrome P450 (CYP) enzymes, in particular the CYP2E1 isozyme, which reduce CCl_4 to CCl_3 and then covert it to superoxides. The oxidative metabolites damage the cell membrane, leading to the cytoplasmic ion imbalance and necrotic cell death. Histological evidence of CCL_4-induced liver damage can be observed mainly in zone 3 of the hepatic acinus [26]. The CCl_4 model of liver injury is one of the most widely used, but unfortunately, in terms of its mechanism of action, it has no direct equivalent in human liver injury. Histopathological changes in acute CCl_4 intoxication are very similar to acetaminophen overdose, which is one of the causes of acute liver injury in humans [27,28]. To induce ALF in mice and rats, the CCl_4 dose should be 40–750 μL per 100 g b.w. [29–31].

D-GalN is a highly hepatospecific compound. Unlike other hepatotoxins, D-GalN does not directly damage other organs and does not cause irritation when injected. In hepatocytes, D-GalN is eliminated by the pathway responsible for galactose metabolism. During the first phase, D-GalN is phosphorylated to galactosamine-1-phosphate (GalN-1-P), then converted to UDP-galactosamine, which has a higher affinity for UDP than for galactose. GalN-1-P is an inhibitor of UDP-glucose pyrophosphorylase-catalysed reaction. Together with UDP, the trapping effect leads to uridine deficiency and inhibition of RNA synthesis. As a consequence, inhibition of protein synthesis leads to apoptotic cell death [32]. In mice and rats, a single D-GalN intraperitoneal injection of 26.6 mg and 20 mg, respectively, changes gene expression related to injury but does not cause visible histopathological changes [33]. Rats are more susceptible to D-GalN intoxication than mice. To develop full-blown acute liver failure, D-GalN dose should be 80–140 mg in rats [34,35] and 150–270 mg per 100 g b.w. in mice [36,37]. Furthermore, the effect of D-GalN intoxication is highly dependent on the animal strain.

In the present pilot study, we compared the dynamics of development of acute liver failure induced in Sprague Dawley rat and BALB/c mouse experimental models by classical hepatotoxins, CCl_4, and D-GalN at doses described as effective [38–40] or modified by us due to excessive mortality in CCl_4-intoxicated mice. We adopted the following criteria of dose selection: signs of acute liver injury in histopathological examination and liver panel; low mortality rate; wide therapeutic window; good animal condition in therapeutic window. We analysed the usefulness of these models with a view to their future introduction into preclinical experiments on stem cell therapy. In particular, it allowed us to identify potential experimental time cut-off points based on histopathological and molecular changes and determine when stem cell therapeutic intervention could be effective as a first-line or adjuvant therapy in the inhibition of progression of these changes in ALF. It is important to define window of treatment in each ALF model, because too late or too early cell implantation could be ineffective in terms of cell homing and suppression of inflammatory reaction and may have negative influence on the final effect of cell therapy.

2. Materials and Methods

2.1 Animals

Six-week-old male BALB/c mice (18–25 g b.w.) and two-month-old male Sprague Dawley rats (180–220 g b.w.) were provided by the Animal House of the Experimental

Table 1. Course of intraperitoneal injections in rats and mice.

Hepatotoxin	Control groups		Acute liver injury	
	Rats	Mice	Rats	Mice
Carbon tetrachloride	Single injection of 400 μL/100 g b.w. olive oil	Single injection of 100 μL/100 g b.w. olive oil	Single injection of 200 μL/100 g b.w.	Single injection of 50 μL/100 g b.w.
D-GalN hydrochloride	Single injection of 500 μL/100 g b.w. saline	Single injection of 250 μL/100 g b.w. saline	Single injection of 50 mg/100 g b.w.	Single injection of 150 mg/100 g b.w.

Animals from experimental groups received hepatotoxin solvents at the same volume as control rats and mice injected with hepatotoxin solutions, saline or olive oil.

Medicine Centre of the Medical University of Silesia and were treated in accordance with the Directive 2010/63/EU on animal experimentation using protocols reviewed and approved by the Local Ethics Committee for Animal Experiments of the Medical University of Silesia (decision no. 18/2018).

Animals (six per cage) were housed under standard conditions of temperature (22 °C $\pm$ 2 °C), humidity (50–60%), light/dark cycle (12 h/12 h), and light intensity (60–400 lux). Water and standard laboratory chow (Labofeed) were available ad libitum.

2.2 Experimental Design

Mice and rats were randomly divided into 8 groups of 12 individuals each. D-galactosamine hydrochloride (Cayman Chemical: 22981) was dissolved in physiological saline. Carbon tetrachloride (Chempur: 118804704) was diluted 1:1 in olive oil (Sigma-Aldrich). The xenobiotics were administered intraperitoneally (i.p.) at the doses shown in Table 1. Animals were not fasted during the experiment. At each of the scheduled time points (12 h, 24 h, 48 h, and day 7), three animals per group were anaesthetized by i.p. injection of 100 mg/kg ketamine and 10 mg/kg xylazine and sacrificed. Blood and tissue samples were taken on the day of anaesthesia. Samples from control groups were collected at the same time after the last saline or oil injection.

2.3 Blood Tests

1 mL of orbital sinus blood was collected to assess liver damage by liver function tests that measured the activity of alanine transaminase (ALT), aspartate transaminase (AST), and alkaline phosphatase (ALP), and total protein (TP). Blood tests were performed by the kinetic method using Chemistry Analyzer (Beckman Coulter: AU480), and reagents and protocols provided by the manufacturer. Blood smears were stained with May Grunwald-Giemsa dye, to assess cell morphology.

2.4 Histopathological Analysis

The liver samples were taken from the left lateral lobe and cut into small pieces, which were fixed in 10% buffered formaline solution, processed using the standard paraffin technique, and stained with haematoxylin and eosin. Liver inflammation was assessed by a simple grading algorithm evaluating parenchymal injury and interface hepatitis. Hepatitis was graded as follows: normal liver parenchyma (0), hepatitis with minimal activity (1), hepatitis with mild activity (2), hepatitis with moderate activity (3), and hepatitis with marked activity and/or multiacinar bridging necrosis (4) [19,20]. Liver steatosis was graded as follows: $<$5% (none; 0), 5–33% (mild; 1), 34–66% (moderate; 2), and $>$67% (severe; 3) [41].

Sirius red staining was performed to differentiate collagen fibres from the background and evaluate the progression of liver fibrosis. Dewaxed, rehydrated, 4-μm-thick liver sections were incubated with Weigert's haematoxylin for 8 min and with picrosirius red in saturated picric acid for 60 min. Finally, they were washed thoroughly with acetic acid and water, covered, and examined under polarized light (Olympus BX-43 polarizer).

To quantify the percentage area occupied by collagen fibres, fifteen random fields of 0.0944 mm^2 from each slide were photographed at 200$\times$ magnification and analysed using ImageJ analysis software (version: 1.53c 26 June 2020, National institutes of Health, Bethesda, Maryland, United States) [42] and the Ishak semi-quantitative scoring system [43,44]. Moreover, the thickness of collagen fibres was evaluated under polarized light using the protocol described by Rich and Whittaker [45].

2.5 Immunohistochemistry

Paraffinized 4-μm-thick rat and mouse liver sections were dewaxed and rehydrated. Endogenous peroxidase activity was quenched with 3% H_2O_2 for 10 min. The sections were immunohistochemically stained to detect Ki-67, a marker of proliferation, and activated caspase-3 (Cas-3), a marker of apoptosis. Liver sections stained with isotype-matched mouse IgG served as negative controls. Immunoreactivity was visualized using diaminobenzidine (Vector Laboratories).

To visualize Ki-67, antigens were retrieved by incubation with citric acid-based antigen unmasking solution (Vector Laboratories) for 60 min. Blocking of non-specific binding was done using 2.5% equine serum (Vector Laboratories) for 60 min. Subsequently, liver sections were incubated with anti-Ki67 (SP6) antibody (ab16667; Abcam) diluted 1:400 for 20 h at 4 °C. Next, the sections were incu-

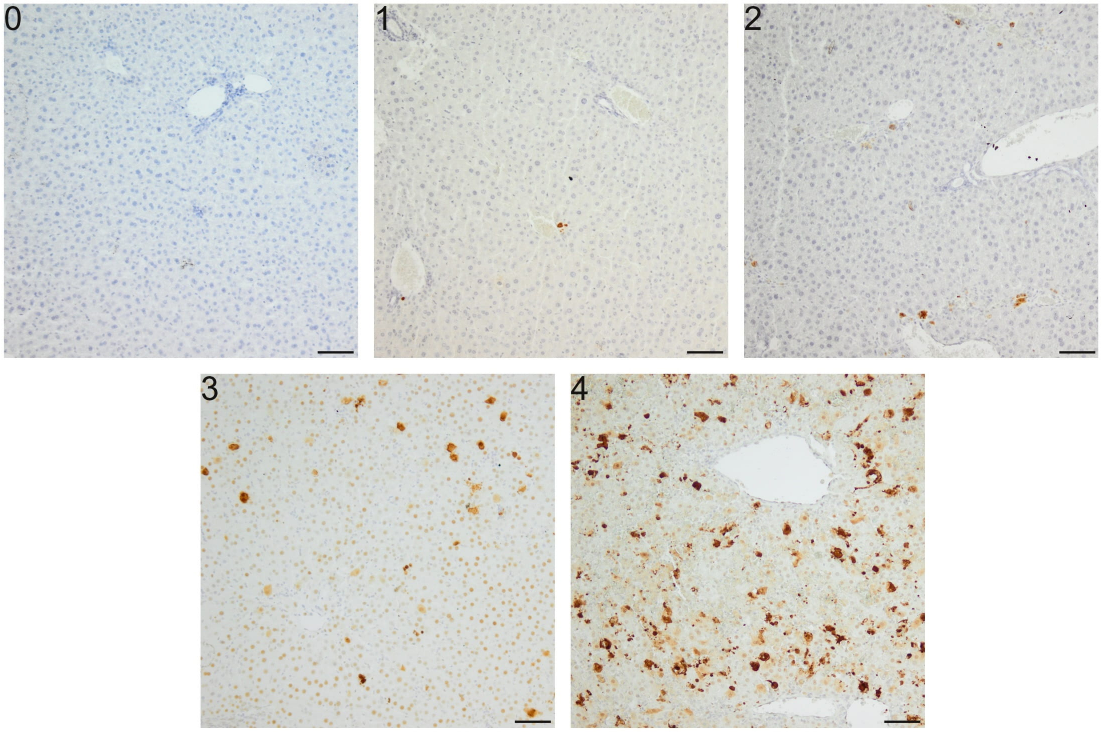

Fig. 1. Semi-quantitative scale for Cas-3 immunoreactivity analysis in apoptosis induced in mice by a single i.p. dose of D-GalN. (0) Lack of positive cells. (1) Few (<10) positive cells per field. (2) 10–25 positive cells per field. (3) 25–50 positive cells per field. (4) >50 positive cells per field; apoptotic cells form clusters. Repeatability of this scoring method was estimated via evaluation of intra- and inter-observer correlation. Intra-observer repeteability was substantial (κ = 0.68), and inter-observer repeteability was moderate (κ = 0.43). A semi-quantitive scale was constructed according to previous recommendations [46]. Mag. 100×, the scale bar represents 50 μm.

bated with anti-rabbit secondary antibody conjugated with peroxidase (Vector Laboratories) at room temperature for 30 min. Sections taken from human tonsil served as positive controls.

Apoptotic cells were identified in the liver slices after 30 min of antigen retrieval and incubation with citric acid-based antigen unmasking solution (Vector Laboratories). Blocking of non-specific binding was done using 5% goat serum (Vector Laboratories). It was followed by incubation with Cas-3 antibody (#9661; Cell Signalling) diluted 1:500 for 20 h at 4 °C. Next, liver slices were incubated with anti-rabbit secondary antibody (Cell Signalling) at 4 °C for 30 min and at room temperature for 30 min.

On each slide, ten random fields of 0.3779 mm^2 each were photographed at a magnification 100 or 200 times. The data were analysed using ImageJ software and expressed as the mean number of positive cells per field of interest (Ki67) or on a semi-quantitative scale (Cas3) (Fig. 1, Ref. [46]).

2.6 RNA Extraction from the Liver

Total RNA was isolated using RNA Extracol reagent (Eurx, Poland) according to the manufacturer's instructions. Tissues were homogenized using Unidrive X 1000 homogenizer (CAT, Germany). Nucleic acid concentration and quality were measured with Nanodrop ND-2000 (Thermo Scientific, USA). RNA was stained with Simply Safe (Eurx, Poland) and visualized after agarose gel electrophoresis.

2.7 Quantitative Real-Time Polymerase Chain Reaction—qRT-PCR

First-strand cDNA synthesis was performed with total RNA and random hexamer primers using smART First Strand cDNA Synthesis Kit (Eurx, Poland) according to the manufacturer's instructions. Reference genes were selected in separate qPCR among HPRT1, TFRC, ACTB, TBP, and PPIH genes for rat samples and among HPRT1, ACTB, GUSB, and PPIH genes for mouse samples. In both cases, ACTB showed a stable expression in the examined samples and was chosen as an endogenous positive control.

The expression of TNFα, IL-6, Gadd45a, COL1A1, COL3A1, TGFβ, CYP2E1, PPARα, C-met, and HGF genes (Table 2, Ref. [47–52]) was detected using FastStart Essential DNA Green Master (Roche, Switzerland) in Light Cycler 96 (Roche, Switzerland). All samples were tested in triplicate. Oligonucleotide primers used for the reactions were purchased from Sigma Aldrich Company (USA). Each run was completed using melting curve analysis to

Table 2. List of genes evaluated in the study.

Gene name	Gene abbreviation	Function	Literature
Tumor necrosis factor alpha Interleukin 6	TNF-α IL-6	Inflammation	[47]
Type I collagen Type III collagen Transforming growth factor beta	COL1A1 COL3A1 TGF-β	Liver fibrosis	[48]
Tyrosine-protein kinase Met Hepatocyte growth factor	C-met HGF	Angiogenesis	[47,49]
Cytochrome P450 2E1	CYP2E1	Oxidative stress	[50]
Peroxisome proliferator-activated receptor alpha	PPAR-α	Lipid metabolism	[51]
Growth arrest and DNA-damage-inducible protein alpha	Gadd45a	Carcinogenesis	[52]

Table 3. Percentage of blood cells determined on routine smears taken from rats and mice intoxicated with CCl_4 and D-GalN.

Time points	Lymphocytes [%]	Monocytes [%]	Eosinophils [%]	Band Neutrophils [%]	Segmented neutrophils [%]
Carbon Tetrachloride Rats					
Control	74 (67–79)	0 (0–0)	6 (3–7)	1 (0–3)	20 (15–25)
12 h	35 (30–36)***	1 (0–2)	0 (0–0)	0 (0–0)	64 (64–68)***
24 h	44 (43–46)**	0 (0–0)	0 (0–0)	0 (0–0)	59 (57–62)**
48 h	74 (73–76)	1 (0–3)	1 (0–2)	2 (1–3)	21 (19–23)
7 d	61 (57–66)	2 (1–4)	0 (0–0)	0 (0–0)	36 (33–39)
Carbon Tetrachloride Mice					
Control	46 (42–47)	0 (0–2)	0 (0–1)	0 (0–1)	53 (50–58)
12 h	36 (26–36)*	0 (0–3)	0 (0–0)	0 (0–0)	64 (61–74)
24 h	11 (8–16)***	1 (0–2)	0 (0–0)	0 (0–0)	88 (82–92)***
48 h	24 (22–31)**	2 (0–3)	0 (0–0)	0 (0–1)	73 (66–78)*
7 d	40 (35–55)	0 (0–0)	0 (0–2)	0 (0–0)	60 (43–65)
D-Galactosamine Rats					
Control	78 (76–88)	0 (0–0)	2 (2–6)	2 (0–5)	15 (8–18)
12 h	58 (52–74)	0 (0–0)	0 (0–0)	0 (0–0)	42 (26–48)*
24 h	63 (48–79)	0 (0–2)	0 (0–1)	0 (0–0)	37 (18–52)
48 h	74 (58–83)	1 (0–5)	2 (1–2)	0 (0–0)	24 (15–35)
7 d	69 (69–69)	3 (3–3)	1 (1–1)	1 (1–1)	26 (26–26)
D-Galactosamine Mice					
Control	62 (48–62)	3 (0–4)	0 (0–2)	0 (0–1)	38 (31–49)
12 h	66 (54–81)	0 (0–1)	0 (0–0)	0 (0–0)	33 (19–46)
24 h	76 (67–85)	0 (0–2)	0 (0–0)	0 (0–1)	24 (15–30)
48 h	68 (67–74)	1 (0–2)	0 (0–0)	0 (0–1)	30 (26–31)
7 d	66 (57–70)	1 (1–2)	0 (0–1)	0 (0–0)	33 (27–42)

Data are presented as median (min–max). No basophils were identified in blood smears; *$p < 0.05$, **$p < 0.01$, ***$p < 0.001$—statistically significant as compared to controls; n = 3.

confirm the specificity of the amplification and the absence of primer dimers. The relative expression of the examined genes was calculated according to the $2^{-\Delta\Delta Ct}$ method.

2.8 Statistical Analysis

Statistical analysis was performed with the STATISTICA 13 software (Version: 13.1, TIBCO Software inc., Palo Alto, CA, USA). If the data were not normally distributed, an appropriate non-parametric Kruskal-Wallis test was used. When the data met the assumptions of normality and variance homogeneity, one-way analysis of variance (ANOVA) with appropriate post-hoc tests were used. For independent groups, Student's *t*-test was also used in justified cases. The statistical significance of differences was set as $p < 0.05$.

3. Results

3.1 Blood Smears and Serum Biochemistry

There were some significant differences in the proportion of lymphocyte and segmented neutrophile subpopulations examined microscopically within the groups of intoxicated rats and mice (Table 3). We observed an upward trend in the number of segmented neutrophils in CCl_4- and D-

Table 4. Changes in the serum parameters of rats and mice intoxicated with CCl_4 and D-GalN.

Time points	Alanine transaminase (ALT) [U/L]	Aspartate transaminase (AST) [U/L]	Alkaline phosphatase (ALP) [U/L]	Total Protein [g/dL]
		Carbon Tetrachloride Rats		
Control	50.7 (49.3–66.2)	201.6 (131.4–260.4)	229.5 (172.5–289.4)	6.2 (5.7–6.3)
12 h	441.2 (413.2–469.1)***	314.6 (234.4–394.7)	241.1 (225.1–358.1)	6.4 (5.8–6.9)
24 h	563.6 (516.3–611.0)***	563.8 (447.5–680.0)*	235.1 (194.6–275.5)	5.5 (5.1–5.9)
48 h	1301 (888.7–1713.3)*	1060.3 (595.7–1524.9)	559 (516.9–601.1)	5.8 (5.7–5.9)
7 d	54.1 (43.9–81.4)#	140.9 (139.3–166.1)	167.2 (163.4–237)	5.9 (5.8–6.5)
		Carbon Tetrachloride Mice		
Control	137.1 (128.5–274)	989 (923.3–1054.7)	65.5 (54–79.3)	4.7 (4.6–5)
12 h	30957.5 (29795–32120)***	21258.5 (20663.5–23761)***	250.2 (151–268)	5.5 (5.1–6)
24 h	31700 (31500–38600)***	3532.5 (3048–4136)**	270.5 (215.4–316.3)	4.8 (4.6–5.3)
48 h	3447.4 (2878.2–3770.3)***	3314.3 (2282.5–4585.6)	288.6 (276.2–295.3)	4.1 (4–4.7)
7 d	61 (30.4–73.2)##	522.5 (429.1–539)#	133.9 (14.4–159.3)	5.1 (4.8–6)
		D-Galactosamine Rats		
Control	51.6 (48.7–61.5)	198.4 (178–220.2)	202 (154.3–268.9)	6.2 (6–6.3)
12 h	415.1 (380.4–719.2)*	476.1 (432.1–611.5)**	227.3 (213.5–376.3)	6.1 (5.5–6.5)
24 h	2509.1 (1889.4–3128.8)*	2280.1 (1721.8–2838.5)*	264.3 (257–474.7)	5.7 (5.6–5.9)
48 h	1833.5 (1707–1960.1)***	1445.8 (1439.7–1452)***	407.7 (357.9–715.9)	5.2 (4.7–5.4)
7 d	58.3 (50.7–66)###	98.3 (88.3–105)###	155.5 (143–199.6)	6.1 (5.8–6.1)
		D-Galactosamine Mice		
Control	143.6 (134.6–206.8)	1049.6 (636–2328.7)	114.3 (105.6–119.6)	4.5 (4.4–5.1)
12 h	176.5 (161.1–207.8)	1057.9 (854.9–1334)	278.2 (235.5–288.4)	5.1 (4.6–6)
24 h	194.7 (162.4–227)	805.9 (715.7–1148.1)	151.4 (150.8–172.1)	4.5 (4.1–4.8)
48 h	187.3 (152.7–221.9)	1054.2 (890.2–1938.6)	155.5 (133.7–168.2)	3.8 (3.5–3.9)
7 d	136 (110.3–138.3)	702.7 (685.9–719.6)	209.3 (205.2–236.3)	4.5 (4.2–5.1)

Data are presented as median (min-max). *$p < 0.05$, **$p < 0.01$, ***$p < 0.001$—statistically significant as compared to controls; #$p < 0.05$, ##$p < 0.01$, ###$p < 0.001$—statistically significant as compared to 48 h; n = 3.

GalN-treated rats at 12 h and 24 h and in CCl_4-treated mice at 24 h and 48 h. These changes were accompanied by decreases in the lymphocyte counts in CCl_4-treated rats (at 12 h and 24 h) and mice (at 12 h, 24 h and 48 h).

We found increasing values of some serum parameters between 12 h and 48 h, namely ALT and AST, mostly in rats and mice intoxicated with CCl_4 and in rats treated with D-GalN (Table 4). In rats treated with CCl_4, we observed elevated activity of ALT, which increased by 8- and 11-fold at 12 h and 24 h, respectively, and by 25-fold at 48 h. In the corresponding group of mice, an increase of ALT was noticed at 12 h (225-fold), 24 h (231-fold), and 48 h (25-fold).

In D-GalN-intoxicated rats, elevated activities of aminotransferases were observed at 12 h (8-fold increase), 24 h (48-fold increase), and 48 h (35-fold increase) for ALT and at 24 h (11-fold increase) and 48 h (7-fold increase) for AST.

Alkaline phosphatase increased especially in CCl_4-treated mice between 12 h and 48 h (3–4 fold) and, to a lower extent, in CCl_4-treated rats (48 h) and D-GalN-treated mice (12 h) and rats (48 h). Total protein concentration remained unchanged in all experimental groups and at all time points (Table 4).

3.2 Histopathological Findings

In the livers of rats treated with CCl_4, we found the first signs of damage 12 h after a single intraperitoneal injection, namely minor infiltration around central veins and ballooning degeneration in hepatocytes of zone 3 of the hepatic acini. The area of liver parenchyma occupied by ballooning degeneration was 8–20% at 12 h, then increased to 20–80% at 24 h, and decreased to 3% at 48 h. Liver necrosis around the central veins occurred 24 h after CCl_4 injection and persisted to 48 h. Liver histology returned to the initial state 7 days after intoxication with the exception of persistent hemosiderin-laden macrophage clusters and a few small lymphocyte clusters (Fig. 2, Table 5).

After a single CCl_4 injection, mouse livers showed moderate inflammatory infiltration and massive pericentral necrosis occupying the area of zone 3, and partially also zone 2, of each hepatic acinus (in total about 60% of the area of the entire acinus), at 12 h, 24 h, and 48 h. At the end of experiment, most of the relevant signs of acute liver

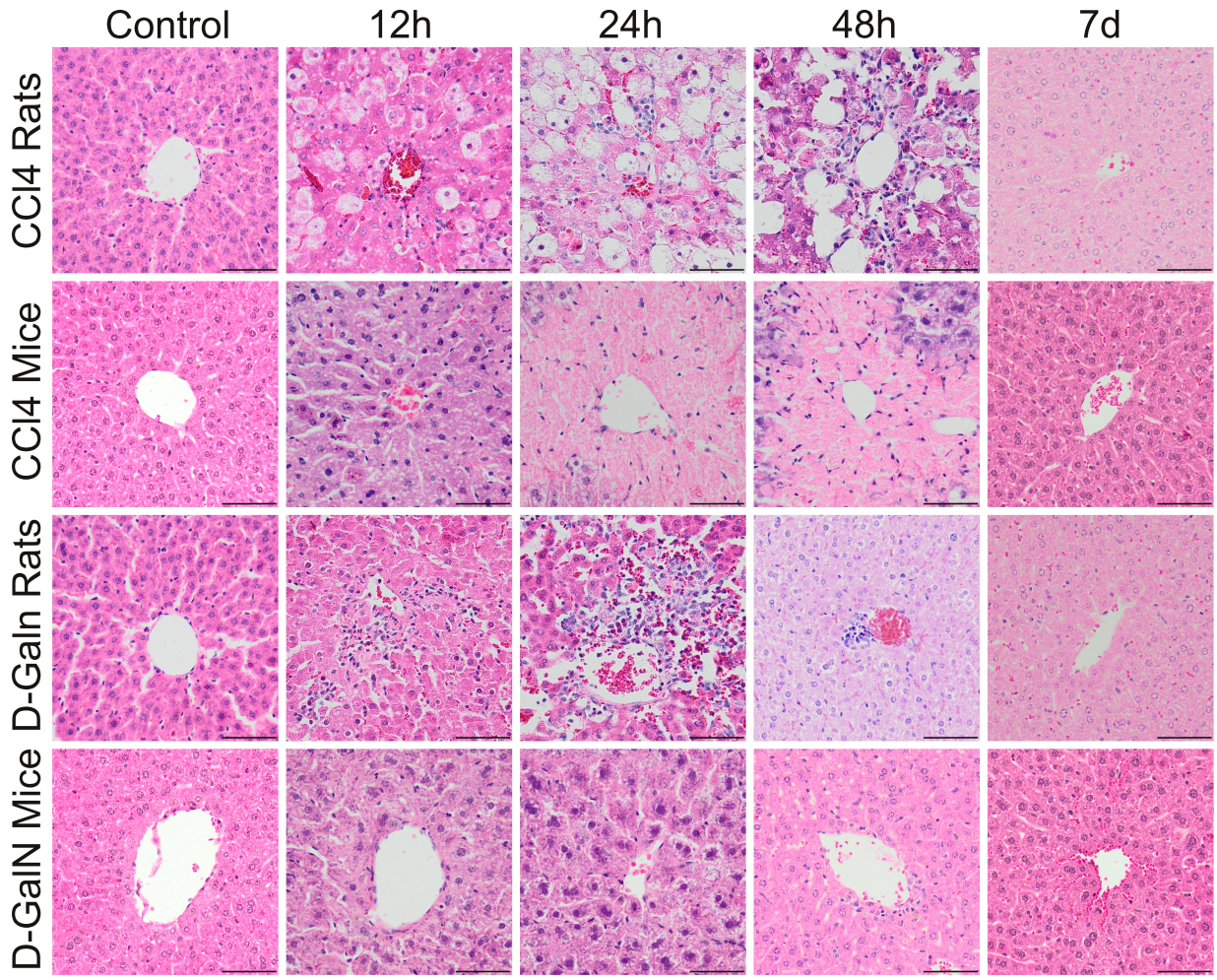

Fig. 2. Histopathological changes in zone 3 of the liver acinus in rats and mice after a single CCl_4or D-GalN injection. In CCl_4 treated rats, pericentral necrosis (pinkish mass) surrounded by foci of ballooning cell degeneration developed around central veins between 12 h and 48 h. In CCl_4 injected mice, massive pericentral necrosis occupying the zone 3, and partially also zone 2 of the liver acici were visible at 24 h and 48 h. In D-GalN administered rats, inflammatory infiltrate around central veins was observed from 12 h, to 48 h. In D-GalN intoxicated mice: only minor pathological changes were observed at 12 h and 24 h around central veins. At the end of observation (7 day) pathological changes were considerably reduced in CCl_4 treated mice and no pathological changes were observed in other groups. Mag. 200×, the scale bar represents 40 μm; H&E staining.

injury receded. There were only a few clusters of lymphocytes around central veins and in periportal areas as well as signs of cholestasis (Fig. 2, Table 5).

In the livers of rats treated with D-GalN, we observed single hepatocyte death, acidophilic bodies, and minor and moderate lymphocytic inflammatory infiltration around central veins after 12 h, 24 h and 48 h. A few lymphocyte and macrophage clusters containing hemosiderin were visible on day 7 (Fig. 2, Table 5).

In D-GalN intoxicated mice, the first histopathological signs of liver injury appeared at 24 h and included small diffuse ballooning degeneration and minor granulocyte infiltration. No pathological changes were observed 7 days after intoxication (Fig. 2, Table 5).

Fibrous expansion corresponding to Ishak stage 1 was observed only in CCl_4–treated mice 7 days after injection (Fig. 3) but not in other experimental groups.

3.3 Proliferation Activity

In CCl_4 intoxicated groups, there was a 4-fold increase in the number of Ki-67+ cells around central veins at 24 h as well as a massive expansion of proliferating parenchymal cells around the portal triads in rats (11-fold) and mice (9-fold) at 48 h (Fig. 4, Table 5).

In D-GalN intoxicated groups, significant increases were observed in the number of Ki-67+ cells around central veins at 12 h and 24 h in rats (4–5-fold) and mice (2-fold). Statistically significant increases were observed in the number of proliferating cells distributed in the hepatic acini at 48 h in rats (13-fold) and mice (3-fold) (Fig. 4, Table 5).

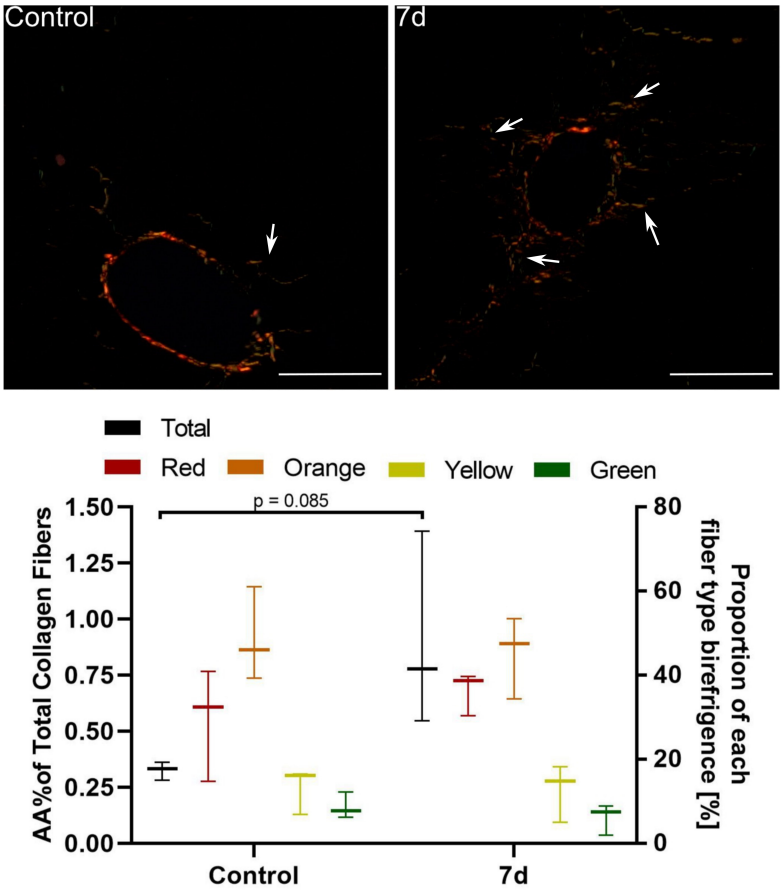

Fig. 3. Assessment of periportal fibrosis in mice 7 d after a single CCl_4 injection. Upper images: Sirius red staining under polarised light. In control mice only thin, individual collagen fibers were observed around portal spaces. 7 d after CCl_4 injection we noted fibrous expansion from portal (and pericentral; not shown) areas visible as numerous short-growing fibrous septa (white arrows) corresponding to Ishak stage 1. Mag. 200×; the scale bar represents 40 μm. Lower graph: Collagen fibre hues under polarized light. Red, orange, yellow, and green indicate their decreasing thickness. The percentage area of collagen fibres increased 2-fold, but it was statistically insignificant; n = 3.

Table 5. Histopathological assessment, cell proliferation activity, and Cas-3 immunoreactivity in the livers of rats and mice intoxicated with CCl_4 and D-GalN.

Time points	Histopathological grading (0–4)		Proliferation activity (positive cells per field)		Cas-3 (0–4)	
	Rats	Mice	Rats	Mice	Rats	Mice
			Carbon Tetrachloride			
Control	0	0	43.5 (22.8–48.8)	43.8 (9.4–45)	0	0
12 h	2	4	94.3 (68.6–341.3)	146.2 (126–148.9)*	1	3
24 h	2	4	181.9 (128.7–235)*	109.2 (84.2–178.4)*	1	0
48 h	4	4	487.8 (395.3–580.2)**	397.8 (270.4–401.9)**	1	1
7 d	0	1	127.5 (33.7–133.7)#	38.6 (29.9–55.2)##	0	2
			D-Galactosamine			
Control	0	0	35.9 (21.3–65.1)	23 (21.6–28.1)	0	0
12 h	2	0	148.1 (147.1–239.4)*	42 (32.2–49.8)*	1	1
24 h	3	0	200.7 (130.2–203.4)**	47.8 (40.4–74)*	2	1
48 h	2	1	477.9 (250.1–579)*	82 (72.3–118.3)**	4	2
7 d	0	0	95.7 (90.8–100.7)#	31.1 (26.3–78.5)	0	0

Histopathological grading and Cas-3 expressions are the median of three animals. Cell proliferation is expressed as the mean number of positive cells per field (min-max). *$p < 0.05$, **$p < 0.01$, ***$p < 0.001$—statistically significant as compared to controls; #$p < 0.05$, ##$p < 0.01$—statistically significant as compared to 48 h.

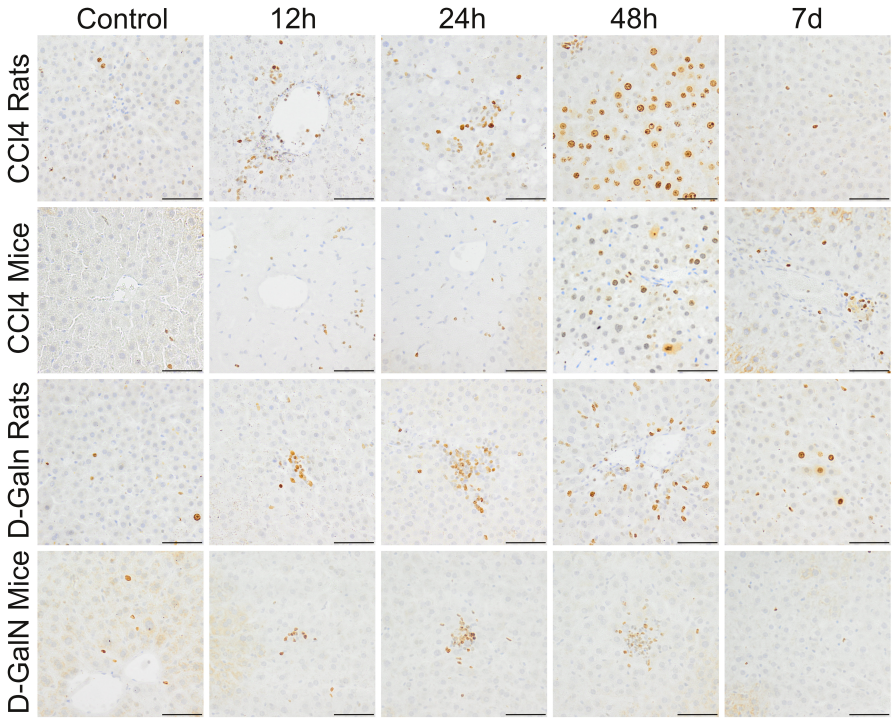

Fig. 4. Ki67+ cells in the livers of rats and mice treated with CCl_4 and D-GalN. Mag. 200×; the scale bar represents 40 μm.

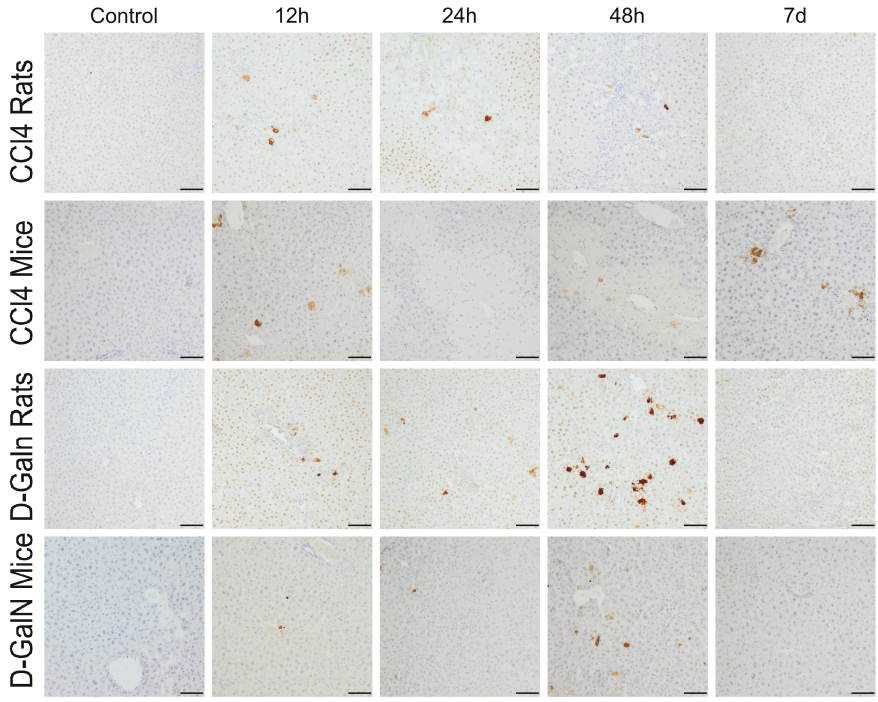

Fig. 5. Immunodetection of apoptotic cells in the liver of rats and mice treated with CCl_4 and D-GalN. Mag. 100×; the scale bar represents 50 μm.

3.4 Cleaved Caspase-3 Expression

In the livers of rats treated with CCl_4 injection, a few Cas-3+ cells were observed at 12 h and 24 h. In mice, 25–50 Cas-3+ cells were localized mainly around the central veins at 12 h, and the number of these cells decreased with time (Fig. 5, Table 5).

In D-GalN-intoxicated animals, a few apoptotic cells were observed at 12 h and 24 h, and their number in the hepatic acini increased significantly at 48 h, especially in rats, and then decreased significantly on day 7 (Fig. 5, Table 5).

3.5 Gene Expression

We observed a similar pattern of COL3A1 expression in rats and mice treated with CCl_4. The expression of COL3A1 showed an upward trend between 12 h and day 7, but the differences were not statistically significant. There were no differences in COL3A1 mRNA expression between time points in rats treated with D-GalN. In D-GalN-treated mice, we observed two peaks: an upregulation at 12 h ($p < 0.05$) and an increase between 24 h and day 7 ($p < 0.05$) (Fig. 6).

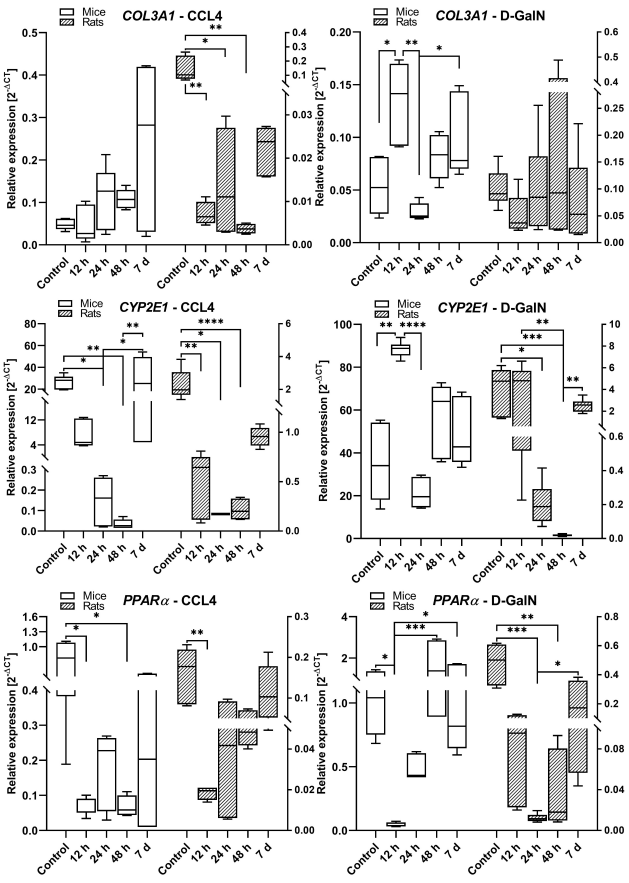

Fig. 6. COL3A1, CYP2E1, and PPARα gene expression in the livers of rats and mice intoxicated with CCl_4 and D-GalN in the ALF model. We observed very low expression of Gadd45a, COL1A1, IL-6, and TNFα in mouse and rat liver samples (data not shown); n = 3.

In CCl_4-treated rats and mice, we observed significantly lower expression of CYP2E1/Cyp2e1 at 12 h ($p < 0.01$), 24 h ($p < 0.05$), and 48 h ($p < 0.0001$) as compared to the control groups and 7-day time point. We also observed a similar pattern of CYP2E1mRNA expression in GalN-intoxicated rats and mice, characterized by decreased levels at 24 h in mice and at 24 h/48 h in rats, and comparable levels between the control and day 7 groups in both species (Fig. 6).

In both rats and mice treated with CCl_4, we observed a significant lowering in PPARα expression at 12 h ($p < 0.01$) in rats and between 12 h and 48 h ($p < 0.05$) in mice. In D-GalN intoxicated rats, PPARα was downregulated at 24 h ($p < 0.001$) and 48 h ($p < 0.01$), whereas in mice it was downregulated at 12 h ($p < 0.05$). In both rats and mice intoxicated with CCl_4 and D-GalN, there were no differences in PPARα expression between the high control and day 7 groups (Fig. 6).

In rats treated with CCl_4, cMET expression showed a downward trend at 12 h, 24 h ($p < 0.05$), and 48 h ($p < 0.01$) as compared with the control group. There was a similar trend in the group of CCl_4-treated mice, but the differences were statistically insignificant. In rats treated with D-GalN, the cMET mRNA expression remained unchanged during the observation with an upward trend at 7 days. However, in mice intoxicated with D-GalN, the cMET expression was upregulated at 48 h ($p < 0.01$) and 7 days ($p < 0.05$) as compared to the control and earlier time points (Fig. 7).

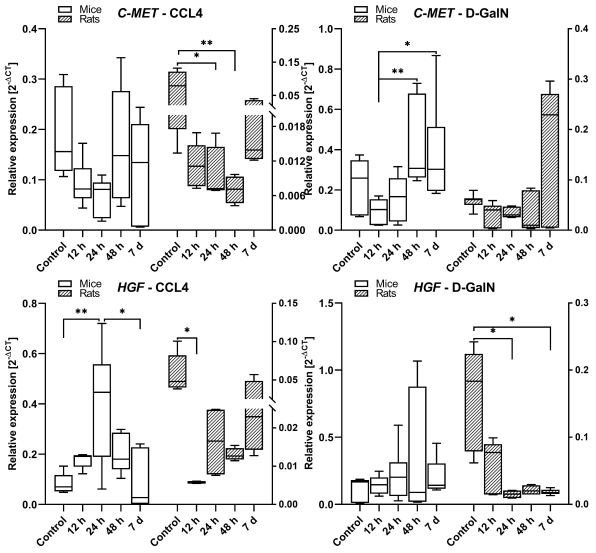

Fig. 7. cMET and HGF gene expression in the livers of rats and mice intoxicated with CCl_4 and D-GalN in the ALF model. n = 3.

In rats treated with CCl_4, the expression of HGF decreased at 12 h ($p < 0.05$), and then showed a statistically insignificant upward trend between 12 h and 7 days. In the corresponding group of mice, the HGF mRNA expression increased at 12 h and 24 h ($p < 0.01$) in comparison to the control and then decreased at 48 h and 7 days ($p < 0.05$). In D-GalN-intoxicated rats, we observed lowered expression of HGF mRNA at 12 h, 24 h, 48 h and 7 days ($p < 0.05$) as compared to the control. In mice intoxicated with D-GalN, the expression of HGF remained unchanged during the observation (Fig. 7).

4. Discussion

There is little information available in the literature describing the toxic effects, including histopathology and gene expression, induced by the classical hepatotoxins CCl_4 and D-GalN in rat and mouse experimental models of hepatotoxicity at early time points in the context of potential cell therapy. In our study we focused on earlier timepoints when the process of liver injury develops, and is not affected by spontaneous recovery of liver acini architecture and function. We wanted to determine experimental time cut-off points for an effective stem cell therapeutic intervention, that should be introduced before pathological changes become advanced or irreversible. Therefore, we analysed the dynamics of ALF development during 48 hours after intoxication with xenobiotic doses described as effective [38–40] or modified by us due to excessive mortality.

In rats treated with a single dose of 200 μL/100g CCl_4, we observed early stages of hepatitis after 12 h, namely ballooning degeneration of hepatocytes, necrosis around central veins, and increased blood parameters. These microscopic observations were similar to those made by Janakat and Al-Merie [40]. The highest activity of aminotransferases and ALP was observed at 48 h after intoxication.

In mice, a dose of CCl_4 that is effective in producing hepatotoxicity can be several times lower than in rats. Doses up to 750 CCl_4 μL/100 g b.w. were described in the literature [29]. High doses were verified by us in preliminary experiments due to mice excessive mortality (about 66%; not published). Finally, in mice treated intraperitoneally with a single injection of 50 μL/100 g CCl_4, we observed rapid development of severe hepatitis with massive parenchymal necrosis in zone 3 of acinus and interface hepatitis, accompanied by highly elevated aminotransferase activities at 12 h. In mice injected with 50 μL/100 g CCl_4, there was a massive liver necrosis observed up to 96 h [29]. At an even higher dose of CCl_4 (100 μL/100g), Yang *et al.* [53] observed parenchyma necrosis as early as 6 h after intoxication and found the largest area of necrosis at 24 h.

A common characteristic of the changes occurring in rats and mice administered with CCl_4 was the rapid progression of histopathological changes in the liver, concentrated mostly in pericentral zone of the liver acini, and signs of toxicity observed in the blood (12 h–24 h). Some of these changes as well as the proliferative activity of the liver cells continued an upward trend in the subsequent period up to 48 h after intoxication. On the other hand, it should be considered that the toxic effect of a single dose of CCl_4 is not permanent in rats and mice and decreases with time after injection [29]. In animals treated with CCl_4, 7 days after intoxication, we did not observe any significant pathological changes except of minor inflammatory infiltrate in mice, which indicates achieving spontaneous recovery in CCl_4 model. Previous data indicated that liver regeneration in this model starts between 72 h and 120 h. Bizzaro *et al.* [29] observed up to 2-fold deacrese in necrotic area at 5th day in comparison to 3rd day of intoxication.

We observed similar trends both in mice and rats in the expression of some important liver genes, i.e., CYP2E1 and PPARα, after a single CCl_4 injection. It is known that a strong inhibitory effect of CCl_4 on cytochrome P450E1 begins from a few minutes [54] to 5–9 h after administration [55]. Inactivation of CYP2E1 during intoxication can be explained by the interaction between cytochrome P450E1 and its substrate - CCl_4. The latter acts as a 'suicide substrate' that causes cytochrome degeneration and the formation of ubiquitin-conjugated microsomal protein [55,56]. We observed this effect of the CCl_4 action as a decrease in CYP2E1 gene expression from 12 h. Furthermore, we observed decreasing PPARα gene expression at the same time. These changes are representative of liver cell injury because both CYP2E1 and PPARα are important components of the hepatic metabolism of drugs and lipids, respectively [57]. Downregulation of PPARα causes more severe steatohepatitis due to impaired lipid metabolism [58]. The changes in gene expression correlated with advanced histopathological changes in the pericentral areas of the liver acini, observed from 12 h to 48 h. Both CYP2E1 and PPARα expression achieved control values on day 7.

We observed a similar pattern of changes (a decrease between 12 h and 48 h/an increase on day 7) induced by CCl_4 in cMet and HGF gene expression in rats and, to a lesser extent, in mice (cMet). HGF is a ligand for the cellular MET (cMet) receptor and together they are responsible for proliferation, cell migration, morphogenesis, angiogenesis, and liver regeneration [59,60]. Overexpression of cMet and HGF can be observed in liver tumours [61]. Our experiments only partially (increased HGF expression in CCl_4-treated mice) corroborate previous results, where liver injury induced by CCl_4 or D-GalN was associated with overexpression of HGF and c-Met [62,63]. Upregulation of HGF gene expression was observed at the early stage of liver failure, and was followed by a drop-off at the late stage [62].

In rats, a dose of D-GalN that can be effective in achieving hepatotoxicity is relatively lower as compared to mice (50 vs 150 mg/100 g). We observed gradually progressing liver injury in rats after a single 50 mg/100 g D-GalN injection. Aminotransferase activity in the blood and apoptosis of liver cells increased gradually between 12 h and 48 h. Our findings on blood parameters are consistent with some other studies confirming that hepatocyte apoptosis is one of the earliest signs of liver injury in the D-GalN model [39]. Apoptotic cells were more numerous than in CCl_4 model. In rats, this was observed in numerous hepatic cells as early as 6 h after 50 mg/100 g GalN injection [39].

In contrast to rat D-GalN model and the rat and mouse CCl_4 model, in mice administered with 150 mg/100 g D-GalN, the first signs of liver injury, such as patches of ballooning degeneration and minor lymphocytic inflamma-

tory infiltrates were visible only at 48 h, but not earlier. Another difference between the D-GalN mouse model and other tested models was that in mice the increases in aminotransferase activities were insignificant, which may indicate a considerably weaker hepatotoxic impact of the administered D-GalN on mice as compared to rats. Different aminotransferase activities observed after 150 mg/100 g D-GalN injection in our study and in some studies by other researches may be due to species-specific sensitivity [38,64,65]. In rats and mice treated with D-GalN, apoptotic activity of hepatocytes intensified gradualy between 24 h and 48 h. Although D-galactosamine is well known to induce apoptosis/necrosis by forming toxic metabolites, also other authors observed rather late apoptotic activity between 48 h and 72 h [64]. These results, together with spontaneous recovery at 7 day, strongly suggest that regeneration phase in this model is shifted to the later time points. Some authors indicate that after D-GalN injection regeneration phase starts at 72 h [66].

In addition to the delayed histopathological signs of liver injury induced in rats and mice by D-GalN, the expression pattern of CYP2E1 and PPARα genes was partially (excluding PPARα genes in rats) shifted to later time points. However, in general this pattern was similar to the corresponding CCl_4 models and was characterized by decreasing expressions at 24 h and/or 48 h, reaching control values after 7 days. Our results are consistent with previous reports, showing that CYP2E1 expression levels decrease 36 h after intoxication and return to normal 1 week after intoxication [67]. Moreover, HGF gene expression was stable in rats and mice between 12 h and 7 days, whereas c-Met expression tended to increase after 48 h, which may be related to the regeneration of the injured liver in this model.

The duration of this short-term experiment was probably not long enough to observe advanced fibrotic changes in the livers of acutely intoxicated rats and mice. The time needed to induce fibrosis in CCl_4 models usually varies from 4–12 weeks, therefore fibrosis-related gene expression and fibrosis-related histopathological changes at early time points after single hepatotoxin injection are not well described in the literature [68,69]. The absence of fibrosis was expected and generally confirmed in this study by histopathological observations and molecular analysis. Nevertheless, as early as day 7, we observed a slight progression in liver fibrosis in histopathological sections, supported by increasing expression of the COL3A1 gene in mice intoxicated with CCl_4. These data are consistent with some previous studies, where after a single or several injections of CCl_4, the researchers obtained a self-limiting fibrosis model characterized by activation of HSCs and upregulation of fibrotic genes [70,71].

The knowledge of ALF dynamics in animal models seems to be crucial in answering the question of when is the best time to intervene with cell therapy and which time cut-off points are most appropriate. Since liver damage progresses rapidly after CCl_4 intoxication, there are basically two approaches to the timing of cell therapy intervention. Based on our findings and the results of some other studies, early intervention to 6 h–12 h seems to be optimal for preventive application of cell therapy [14,72]. Therapeutic intervention during this time seems to be most effective due to the likely mechanism of suppression of the inflammatory process at its early stage. However, cell implantation shortly after intoxication may expose these cells to the toxic effects of the administrated xenobiotic. Due to the ability of CCl_4 to create free radicals, the risk of interaction between CCl_4 and stem cells is high, especially if the routes of cells and hepatotoxin administration are the same [73]. Unlike CCl_4, D-GalN does not directly damage cells other than hepatocytes, so the risk of a negative interaction between D-GalN and the injected cells is lower.

It is very common for researchers to perform cell therapy 24 h or 48 h after CCl_4 administration [74–77]. However, after this period, we observed severe histopathological changes in mice and rats, corresponding to the acute phase of full-blown liver failure. Cell implantation at the above-mentioned time points could potentially increase the regenerative potential of the liver and shorten the recovery period. Cell administration between 24 h and 48 h seems to be more related to clinical practice, where therapeutic intervention coincides with the diagnosis of full-blown liver failure.

The D-GalN liver injury model is characterized by a longer time (especially in mice—up to 48 h) between toxin injection and the phase of full-blown hepatitis. This provides a wide therapeutic window for cell therapy intervention. In this model, cell therapy is usually conducted prior to development of full-blown liver failure, 24 h after intoxication [13,78,79].

5. Conclusions

In conclusion, we propose the following potential experimental time points appropriate for cell therapy intervention in animal models of CCl_4 and D-GalN-dependent acute liver failure: rat and mouse CCl_4 model—12 h, rat D-GalN model—24 h, and mouse D-GalN model—48 h. In the presented models, cell administration seems to be ineffective after 48 h due to the self-limiting properties of liver injury and spontaneous liver parenchyma regeneration after this time point.

Abbreviations

CCl_4, Carbon tetrachloride; D-GalN, D-galactosamine; ALF, acute liver failure; i.p., intraperitoneal; ALT, alanine transaminase; AST, aspartate transaminase; ALP, alkaline phosphatase; TP, total protein; Cas-3, Cleaved Caspase 3; TNF-α, Tumor necrosis factor alpha; IL-6, Interleukin 6; COL1A1, Type I collagen; COL3A1, Type III collagen; TGF-β, Transforming growth factor beta; C-met, Tyrosine-protein kinase Met; HGF,

Hepatocyte growth factor; CYP2E1, Cytochrome P450 2E1; PPAR-α, Peroxisome proliferator-activated receptor alpha.

Author Contributions

PC and MK designed the research study. PC supported the studies financially (grands), provided help and advice. MK, ŁL, EK, AS-S, EB, MH, MM, BS, AP, AG, JP performed the research. PC, MK, ŁL, AS-S, BS analyzed the data. PC, MK, AS-S wrote the manuscript. All authors contributed to editorial changes in the manuscript. All authors read and approved the final manuscript.

Ethics Approval and Consent to Participate

Animal experiments were approved by the Animal Experiments Ethical Committee of Medical University of Silesia, Katowice, Poland (decision no. 18/2018).

Acknowledgment

We thank the Silesian Analytical Laboratory (Katowice; Poland) for performing serum biochemistry analysis and blood morphology assessment. We thank Katarzyna Lorek from Students Scientific Society SUM Katowice for her participation in administration of xenobiotics to laboratory animals.

Funding

The studies were supported by institutional grands (SUM Katowice) no: KNW-1-103/N/8/0 and KNW-1-100/K/9/0.

Conflict of Interest

The authors declare no conflict of interest.

References

[1] Mathai S, Panackel C, Thomas R, Sebastian B. Recent advances in management of acute liver failure. Indian Journal of Critical Care Medicine. 2015; 19: 27–33.

[2] Fontana RJ. Acute Liver Failure Including Acetaminophen Overdose. Medical Clinics of North America. 2008; 92: 761–794.

[3] Wendon J, Cordoba J, Dhawan A, Larsen FS, Manns M, Nevens F, *et al*. EASL Clinical Practical Guidelines on the management of acute (fulminant) liver failure. Journal of Hepatology. 2017; 66: 1047–1081.

[4] Gotthardt D, Riediger C, Weiss KH, Encke J, Schemmer P, Schmidt J, *et al*. Fulminant hepatic failure: etiology and indications for liver transplantation. Nephrology, Dialysis, Transplantation. 2007; 22: viii5–viii8.

[5] Castaldo ET, Chari RS. Liver transplantation for acute hepatic failure. HPB. 2006; 8: 29–34.

[6] Mendizabal M. Liver transplantation in acute liver failure: a challenging scenario. World Journal of Gastroenterology. 2016; 22: 1523–1531.

[7] Kantola T, Ilmakunnas M, Koivusalo A, Isoniemi H. Bridging Therapies and Liver Transplantation in Acute Liver Failure; 10 Years of MARS Experience from Finland. Scandinavian Journal of Surgery. 2011; 100: 8–13.

[8] Michalik M, Gładyś A, Czekaj P. Differentiation of Cells Isolated from Afterbirth Tissues into Hepatocyte-Like Cells and their Potential Clinical Application in Liver Regeneration. Stem Cell Reviews and Reports. 2021; 17: 581–603.

[9] Lim R, Malhotra A, Tan J, Chan ST, Lau S, Zhu D, *et al*. First-in-Human Administration of Allogeneic Amnion Cells in Premature Infants with Bronchopulmonary Dysplasia: a Safety Study. Stem Cells Translational Medicine. 2018; 7: 628–635.

[10] Melville JM, McDonald CA, Bischof RJ, Polglase GR, Lim R, Wallace EM, *et al*. Human amnion epithelial cells modulate the inflammatory response to ventilation in preterm lambs. PLoS ONE. 2017; 12: e0173572.

[11] Kolanko E, Grajoszek A, Czekaj P. Immunosuppressive Potential of Activated Human Amniotic Cells in an Experimental Murine Model of Skin Allo- and Xenotransplantation. Frontiers in Medicine. 2021; 8: 715590.

[12] Li Y, Zhang C, Sheng Q, Bai H, Ding Y, Dou X. Mesenchymal stem cells rescue acute hepatic failure by polarizing M2 macrophages. World Journal of Gastroenterology. 2017; 23: 7978–7988.

[13] Ramanathan R, Rupert S, Selvaraj S, Satyanesan J, Vennila R, Rajagopal S. Role of Human Wharton's Jelly Derived Mesenchymal Stem Cells (WJ-MSCs) for Rescue of d - Galactosamine Induced Acute Liver Injury in Mice. Journal of Clinical and Experimental Hepatology. 2017; 7: 205–214.

[14] Liu Q, Liu Q, Li J, Wei L, Ren K, Zhang X, *et al*. Therapeutic efficiency of human amniotic epithelial stem cell-derived functional hepatocyte-like cells in mice with acute hepatic failure. Stem Cell Research & Therapy. 2018; 9: 321.

[15] Nagamoto Y, Takayama K, Ohashi K, Okamoto R, Sakurai F, Tachibana M, *et al*. Transplantation of a human iPSC-derived hepatocyte sheet increases survival in mice with acute liver failure. Journal of Hepatology. 2016; 64: 1068–1075.

[16] Baumgartner D, LaPlante-O'Neill PM, Sutherland DE, Najarian JS. Effects of intrasplenic injection of hepatocytes, hepatocyte fragments and hepatocyte culture supernatants on D-galactosamine-induced liver failure in rats. European Surgical Research. 1983; 15: 129–135.

[17] Lin N, Wu H, Ho JH, Liu C, Lee OK. Mesenchymal stem cells prolong survival and prevent lethal complications in a porcine model of fulminant liver failure. Xenotransplantation. 2019; 26: e12542.

[18] Zhang Y, Cai W, Huang Q, Gu Y, Shi Y, Huang J, *et al*. Mesenchymal stem cells alleviate bacteria-induced liver injury in mice by inducing regulatory dendritic cells. Hepatology. 2014; 59: 671–682.

[19] Zhang Q, Huang Y, Sun J, Gu T, Shao X, Lai D. Immunomodulatory effect of human amniotic epithelial cells on restoration of ovarian function in mice with autoimmune ovarian disease. Acta Biochimica et Biophysica Sinica. 2019; 51: 845–855.

[20] Lim R, Hodge A, Moore G, Wallace EM, Sievert W. A Pilot Study Evaluating the Safety of Intravenously Administered Human Amnion Epithelial Cells for the Treatment of Hepatic Fibrosis. Frontiers in Pharmacology. 2017; 8: 549.

[21] Huang B, Cheng X, Wang H, Huang W, la Ga Hu Z, Wang D, *et al*. Mesenchymal stem cells and their secreted molecules predominantly ameliorate fulminant hepatic failure and chronic liver fibrosis in mice respectively. Journal of Translational Medicine. 2016; 14: 45.

[22] Anger F, Camara M, Ellinger E, Germer C, Schlegel N, Otto C, *et al*. Human Mesenchymal Stromal Cell-Derived Extracellular Vesicles Improve Liver Regeneration after Ischemia Reperfusion Injury in Mice. Stem Cells and Development. 2019; 28: 1451–1462.

[23] Czekaj P, Król M, Limanówka Ł, Michalik M, Lorek K, Gramignoli R. Assessment of animal experimental models of

toxic liver injury in the context of their potential application as preclinical models for cell therapy. European Journal of Pharmacology. 2019; 861: 172597.
[24] McGill MR, Jaeschke H. Animal models of drug-induced liver injury. Biochimica Et Biophysica Acta (BBA) - Molecular Basis of Disease. 2019; 1865: 1031–1039.
[25] Fahmy SR, Hamdi SAH, Abdel-Salam HA. Curative effect of dietary freshwater and marine crustacean extracts on carbon tetrachloride-induced nephrotoxicity. Australian Journal of Basic and Applied Sciences. 2009; 3: 2118–2129.
[26] Apte U. Models to Study Liver Regeneration. Liver regeneration: basic mechanisms, relevant models and clinical applications (pp. 15–40). Elsevier/Academic Press: Kansas City, United States. 2015.
[27] Yan M, Huo Y, Yin S, Hu H. Mechanisms of acetaminophen-induced liver injury and its implications for therapeutic interventions. Redox Biology. 2018; 17: 274–283.
[28] Blazka ME, Elwell MR, Holladay SD, Wilson RE, Luster MI. Histopathology of acetaminophen-induced liver changes: role of interleukin 1 alpha and tumor necrosis factor alpha. Toxicologic Pathology. 1996; 24: 181–189.
[29] Bizzaro D, Crescenzi M, Di Liddo R, Arcidiacono D, Cappon A, Bertalot T, *et al*. Sex-dependent differences in inflammatory responses during liver regeneration in a murine model of acute liver injury. Clinical Science. 2018; 132: 255–272.
[30] Ustuner D, Colak E, Dincer M, Tekin N, Burukoglu Donmez D, Akyuz F, *et al*. Posttreatment Effects of Olea Europaea L. Leaf Extract on Carbon Tetrachloride-Induced Liver Injury and Oxidative Stress in Rats. Journal of Medicinal Food. 2018; 21: 899–904.
[31] Zarezade V, Moludi J, Mostafazadeh M, Mohammadi M, Veisi A. Antioxidant and hepatoprotective effects of *Artemisia dracunculus* against CCl_4-induced hepatotoxicity in rats. Avicenna Journal of Phytomedicine. 2018; 8: 51–62.
[32] Decker K, Keppler D. Galactosamine hepatitis: key role of the nucleotide deficiency period in the pathogenesis of cell injury and cell death. Reviews of Physiology Biochemistry and Pharmacology. 1974; 77–106.
[33] Galun E, Zeira E, Pappo O, Peters M, Rose-John S. Liver regeneration induced by a designer human IL-6/sIL-6R fusion protein reverses severe hepatocellular injury. The FASEB Journal. 2000; 14: 1979–1987.
[34] Babu PR, Bhuvaneswar C, Sandeep G, Ramaiah CV, Rajendra W. Hepatoprotective role of Ricinus communis leaf extract against D-galactosamine induced acute hepatitis in albino rats. Biomedicine & Pharmacotherapy. 2017; 88: 658–666.
[35] Zhang Y. Improved prescription of taohechengqi-tang alleviates D-galactosamine acute liver failure in rats. World Journal of Gastroenterology. 2016; 22: 2558–2565.
[36] Drucker C, Rabe B, Chalaris A, Schulz E, Scheller J, Rose-John S. Interleukin-6 trans-signaling regulates glycogen consumption after D-galactosamine-induced liver damage. Journal of Interferon and Cytokine Research. 2009; 29: 711–718.
[37] Lu Y, Wang WJ, Song YZ, Liang ZQ. The protective mechanism of schisandrin A in d-galactosamine-induced acute liver injury through activation of autophagy. Pharmaceutical Biology. 2014; 52: 1302–1307.
[38] Tsutsui S, Hirasawa K, Takeda M, Itagaki S, Kawamura S, Maeda K, *et al*. Apoptosis of Murine Hepatocytes Induced by High Doses of Galactosamine. Journal of Veterinary Medical Science. 1997; 59: 785–790.
[39] Catal T, Bolkent S. Combination of Selenium and Three Naturally Occurring Antioxidants Administration Protects d-Galactosamine-Induced Liver Injury in Rats. Biological Trace Element Research. 2008; 122: 127–136.
[40] Janakat S, Al-Merie H. Optimization of the dose and route of injection, and characterisation of the time course of carbon tetrachloride-induced hepatotoxicity in the rat. Journal of Pharmacological and Toxicological Methods. 2002; 48: 41–44.
[41] Bingül İ, Aydın AF, Başaran-Küçükgergin C, Doğan-Ekici I, Çoban J, Doğru-Abbasoğlu S, *et al*. High-fat diet plus carbon tetrachloride-induced liver fibrosis is alleviated by betaine treatment in rats. International Immunopharmacology. 2016; 39: 199–207.
[42] Schindelin J, Arganda-Carreras I, Frise E, Kaynig V, Longair M, Pietzsch T, *et al*. Fiji: an open-source platform for biological-image analysis. Nature Methods. 2012; 9: 676–682.
[43] Standish RA, Cholongitas E, Dhillon A, Burroughs AK, Dhillon AP. An appraisal of the histopathological assessment of liver fibrosis. Gut. 2006; 55: 569–578.
[44] Krishna M. Histological Grading and Staging of Chronic Hepatitis. Clinical Liver Disease. 2021; 17: 222–226.
[45] Rich L, Whittaker P. Collagen and picosirius red staining: A poalrized light assessment of fibrillar hue and spatioal distribution. Journal of Morphology. 2005; 22: 97–104.
[46] Gibson-Corley KN, Olivier AK, Meyerholz DK. Principles for Valid Histopathologic Scoring in Research. Veterinary Pathology. 2013; 50: 1007–1015.
[47] Giebeler A, Boekschoten MV, Klein C, Borowiak M, Birchmeier C, Gassler N, *et al*. C-Met Confers Protection against Chronic Liver Tissue Damage and Fibrosis Progression after Bile Duct Ligation in Mice. Gastroenterology. 2009; 137: 297–308.e3084.
[48] Bai Q, Yan H, Sheng Y, Jin Y, Shi L, Ji L, *et al*. Long-term acetaminophen treatment induced liver fibrosis in mice and the involvement of Egr-1. Toxicology. 2017; 382: 47–58.
[49] Vasir B, Reitz P, Xu G, Sharma A, Bonner-Weir S, Weir GC. Effects of diabetes and hypoxia on gene markers of angiogenesis (HGF, cMET, uPA and uPAR, TGF-alpha, TGF-beta, bFGF and Vimentin) in cultured and transplanted rat islets. Diabetologia. 2000; 43: 763–772.
[50] Sutti S, Rigamonti C, Vidali M, Albano E. CYP2E1 autoantibodies in liver diseases. Redox Biology. 2014; 3: 72–78.
[51] Montagner A, Polizzi A, Fouché E, Ducheix S, Lippi Y, Lasserre F, *et al*. Liver PPARα is crucial for whole-body fatty acid homeostasis and is protective against NAFLD. Gut. 2016; 65: 1202–1214.
[52] Hong L, Sun Q, Xu T, Wu Y, Zhang H, Fu R, *et al*. New role and molecular mechanism of Gadd45a in hepatic fibrosis. World Journal of Gastroenterology. 2016; 22: 2779.
[53] Yang Y, Zhai H, Wan Y, Wang X, Chen H, Dong L, *et al*. Recombinant Human HPS Protects Mice and Nonhuman Primates from Acute Liver Injury. International Journal of Molecular Sciences. 2021; 22: 12886.
[54] Knockaert L, Berson A, Ribault C, Prost P, Fautrel A, Pajaud J, *et al*. Carbon tetrachloride-mediated lipid peroxidation induces early mitochondrial alterations in mouse liver. Laboratory Investigation. 2012; 92: 396–410.
[55] Tierney DJ, Haas AL, Koop DR. Degradation of cytochrome P450 2E1: Selective loss after labilization of the enzyme. Archives of Biochemistry and Biophysics. 1992; 293: 9–16.
[56] Dai Y, Cederbaum AI. Inactivation and degradation of human cytochrome P4502E1 by CCl4 in a transfected HepG2 cell line. Journal of Pharmacology and Experimental Therapeutics. 1995; 275: 1614–1622.
[57] Aristatile B, Al-Assaf AH, Pugalendi KV. Carvacrol ameliorates the PPAR-A and cytochrome P450 expression on D-galactosamine induced hepatotoxicity rats. African Journal of Traditional, Complementary and Alternative Medicines. 2014; 11: 118–123.
[58] Eslam M, Khattab MA, Harrison SA. Peroxisome proliferator-activated receptors and hepatitis C virus. Therapeutic Advances in Gastroenterology. 2011; 4: 419–431.

[59] Wang H, Rao B, Lou J, Li J, Liu Z, Li A, *et al*. The Function of the HGF/c-Met Axis in Hepatocellular Carcinoma. Frontiers in Cell and Developmental Biology. 2020; 8: 55.
[60] Otsuka T, Takagi H, Horiguchi N, Toyoda M, Sato K, Takayama H, *et al*. CCl4-induced acute liver injury in mice is inhibited by hepatocyte growth factor overexpression but stimulated by NK2 overexpression. FEBS Letters. 2002; 532: 391–395.
[61] Nakayama N, Kashiwazaki H, Kobayashi N, Hamada J, Ogiso Y, Itakura Y, *et al*. Hepatocyte growth factor and c-met expression in Long-Evans Cinnamon rats with spontaneous hepatitis and hepatoma. Hepatology. 1996; 24: 596–602.
[62] Cramer T, Schuppan D, Bauer M, Pfander D, Neuhaus P, Herbst H. Hepatocyte growth factor and c-Met expression in rat and human liver fibrosis. Liver International. 2004; 24: 335–344.
[63] Shiota G, Okano J, Kawasaki H, Kawamoto T, Nakamura T. Serum hepatocyte growth factor levels in liver diseases: Clinical implications. Hepatology. 1995; 21: 106–112.
[64] Drucker C, Gewiese J, Malchow S, Scheller J, Rose-John S. Impact of interleukin-6 classic- and trans-signaling on liver damage and regeneration. Journal of Autoimmunity. 2010; 34: 29–37.
[65] Tsuji T, Shinohara T. Pathological study of chronic d-galactosamine induced hepatitis in mice by administration of adjuvants an animal model of the chronic active hepatitis. Gastroenterologia Japonica. 1981; 16: 9–20.
[66] Chung H, Kim H, Jang K, Kim M, Yang J, Kang K, *et al*. Comprehensive analysis of differential gene expression profiles on d-galactosamine-induced acute mouse liver injury and regeneration. Toxicology. 2006; 227: 136–144.
[67] Asaoka Y, Sakai H, Takahashi N, Hirata A, Tsukamoto T, Yamamoto M, *et al*. Intraperitoneal injection ofd-galactosamine provides a potent cell proliferation stimulus for the detection of initiation activities of chemicals in rat liver. Journal of Applied Toxicology. 2005; 25: 554–561.
[68] Zhang Y, Miao H, Yan H, Sheng Y, Ji L. Hepatoprotective effect of Forsythiae Fructus water extract against carbon tetrachloride-induced liver fibrosis in mice. Journal of Ethnopharmacology. 2018; 218: 27–34.
[69] Jiang W, Tan Y, Cai M, Zhao T, Mao F, Zhang X, *et al*. Human Umbilical Cord MSC-Derived Exosomes Suppress the Development of CCl4-Induced Liver Injury through Antioxidant Effect. Stem Cells International. 2018; 2018: 6079642.
[70] Constandinou C, Henderson N, Iredale JP. Modeling liver fibrosis in rodents. Methods in Molecular Medicine. 2005; 117: 237–250.
[71] Oakley F, Trim N, Constandinou CM, Ye W, Gray AM, Frantz G, *et al*. Hepatocytes Express Nerve Growth Factor during Liver Injury: evidence for paracrine regulation of hepatic stellate cell apoptosis. The American Journal of Pathology. 2003; 163: 1849–1858.
[72] Yukawa H, Noguchi H, Oishi K, Takagi S, Hamaguchi M, Hamajima N, *et al*. Cell Transplantation of Adipose Tissue-Derived Stem Cells in Combination with Heparin Attenuated Acute Liver Failure in Mice. Cell Transplantation. 2009; 18: 611–618.
[73] Ren X, Xin L, Zhang M, Zhao Q, Yue S, Chen K, *et al*. Hepatoprotective effects of a traditional Chinese medicine formula against carbon tetrachloride-induced hepatotoxicity in vivo and in vitro. Biomedicine & Pharmacotherapy. 2019; 117: 109190.
[74] Gruttadauria S, Grosso G, Pagano D, Biondi A, Echeverri GJ, Seria E, *et al*. Marrow-Derived Mesenchymal Stem Cells Restore Biochemical Markers of Acute Liver Injury in Experimental Model. Transplantation Proceedings. 2013; 45: 480–486.
[75] Putra A, Rosdiana I, Darlan DM, Alif I, Hayuningtyas F, Wijaya I, *et al*. Intravenous Administration is the Best Route of Mesenchymal Stem Cells Migration in Improving Liver Function Enzyme of Acute Liver Failure. Folia Medica. 2020; 62: 52–58.
[76] Varaa N, Azandeh S, Khorsandi L, Bijan Nejad D, Bayati V, Bahreini A. Ameliorating effect of encapsulated hepatocyte-like cells derived from umbilical cord in high mannuronic alginate scaffolds on acute liver failure in rats. Iranian Journal of Basic Medical Sciences. 2018; 21: 928–935.
[77] Li D, Fan J, He X, Zhang X, Zhang Z, Zeng Z, *et al*. Therapeutic effect comparison of hepatocyte-like cells and bone marrow mesenchymal stem cells in acute liver failure of rats. International Journal of Experimental Pathology. 2015; 8: 11–24.
[78] Wang J, Ren H, Yuan X, Ma H, Shi X, Ding Y. Interleukin-10 secreted by mesenchymal stem cells attenuates acute liver failure through inhibiting pyroptosis. Hepatology Research. 2018; 48: E194–E202.
[79] Lam SP, Luk JM, Man K, Ng KT, Cheung CK, Rose-John S, *et al*. Activation of interleukin-6-induced glycoprotein 130/signal transducer and activator of transcription 3 pathway in mesenchymal stem cells enhances hepatic differentiation, proliferation, and liver regeneration. Liver Transplantation. 2010; 16: 1195–1206.